Technical Addendum to the Winningsplan Groningen 2016

Production, Subsidence, Induced Earthquakes and Seismic Hazard and Risk Assessment in the Groningen Field

Part II
Subsidence

The report “Technical Addendum to the Winningsplan Groningen 2016 - Production, Subsidence, Induced Earthquakes and Seismic Hazard and Risk Assessment in the Groningen Field” consists of five separate documents:

Document 1	Chapters 1 to 5;	Summary and Production
Document 2	Chapter 6;	Subsidence
Document 3	Chapter 7;	Hazard
Document 4	Chapter 8;	Risk
Document 5	Chapter 9;	Damage and Appendices.

Each of these documents is also available as a *.pdf file of a size smaller than 10Mbyte, allowing sharing through e-mail.

Table of Contents

6 Subsidence

6.1 Summary

This chapter presents in more technical detail the subsidence forecasts as presented in chapter 5 of the Groningen winningsplan. Land subsidence above the Groningen field is caused by compaction of the reservoir due to the gas production. In a first order approach the compaction in the reservoir can be calculated by multiplying the depleting thickness, the amount of depletion (or pressure drop) and the compressibility of the rock. Geodetic information above the field indicates however that the relationship between pressure drop and subsidence is not simply linear. The most logical explanation for this phenomenon is believed to be a more complex compaction behavior of the reservoir.

Therefore two compaction models are investigated for the Groningen subsidence calculations, both describing a non-linear relationship with pressure drop, i.e. the time decay (NAM, 2011) model and the rate type compaction isotach model (RTCiM, TNO2013). The time decay model, according to which compaction decays with time after a pressure perturbation, has been adopted in NAM for subsidence calculations since 2011.

Typically geodetic observations above the gas fields in The Netherlands show an increase of the subsidence rate after the first years of production. The first model used to match this observation was a bi-linear compaction model and this was used by NAM till 2011. However, when updating the Ameland winningsplan in 2010 it became apparent that the bi-linear model could not describe the ongoing subsidence observed above this field (NAM, 2011) with the decreasing depletion rate at the end of field life. An updated model to address this delayed subsidence both at the start and at the end of the production was adopted: the time decay compaction model. The time decay model has less free parameters than the bi-linear model while matching the full geodetic dataset above the field of Ameland using the compressibility (Cm)-porosity relation based on laboratory data.

A similar approach was followed for matching the subsidence above the Groningen field but in this case the aforementioned Cm-porosity trend line could not be used directly. A calibration factor of about 0.5 had to be applied to this trend line in order to obtain a good temporal and spatial match between modelled and measured subsidence. For the 2016 winningsplan, supported by this document, a spatially varying Cm value derived from a direct inversion of the geodetic data was used to further improve the match.

Besides the application of the time decay model, a second model was adopted from TNO (TNO, 2013), i.e. the RTCiM model. This model also provides a good match with the historical subsidence data but contains more degrees of freedom when compared to the time decay model.

Reservoir pressures from the Groningen MoReS model have been used as input for the compaction model. The distribution of reservoir porosity and thickness were taken from the static Petrel model and upscaled with the condition that the upscaled compaction be equal to the sum of the compaction of the individual layers.

A RMS method was used to check the “goodness-of-fit” between modelled and measured historic subsidence.

6.2 Introduction

The Groningen field was discovered in 1959 and gas production started in 1963. Globally, the field belongs to the top-ten largest gas fields. Subsidence was recognised as a risk before production began and was monitored from the start through regular levelling surveys. Since 1993 also satellite based Interferometric Synthetic Aperture Radar (InSAR) measurements have been used for this purpose. In 2013 the first continuous GPS monitoring station in Groningen was installed in Ten Post.

The subsidence models were revised and refined through time as more data became available. Compaction models have to meet two basic criteria: they have to closely match the subsidence measurements and they should be based on plausible physical mechanisms. Section 6.3 will describe the availability of data, i.e., laboratory compaction data and geodetic data. Section 6.4 describes the geomechanics of the Groningen field including the compaction models and the importance of overburden behaviour. Subsequent sections (6.5 and 6.6) describe model calibration and the subsidence forecasts.

6.3 Geodetic and geomechanical data

This section describes two sources of data relevant for model calibration. First, an overview will be presented of the geodetic data, followed by a description of the geomechanical data (Cm measurements). Other data such as geological data and pressure data have been described in Part I of this Technical Addendum.

6.3.1 Survey protocol

The Dutch mining law (from 2002) requires that a survey plan is in place for all onshore gas and oil production activities. The State Supervision of Mines (Staatstoezicht op de Mijnen, SodM) has to be informed every year on the status of the survey plan, on any changes made to the plan, and on the geodetic surveys scheduled for the coming year.

For Groningen, a full levelling survey has to be carried out every 5 years.

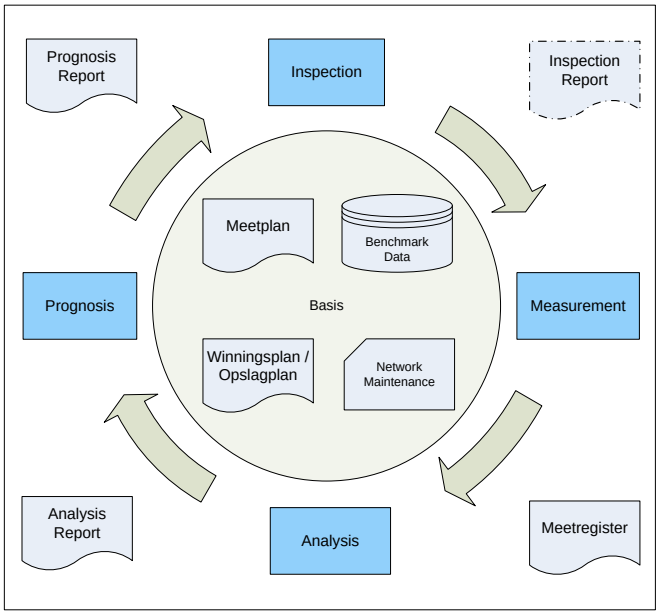

Figure 6-1 Schematic overview of a measurement and control workflow that is embedded in all Dutch production plans

An initial survey for Groningen was carried out in 1964, but only covered the southern part of the field. The first full levelling survey covering the entire area was in 1972. The latest survey procedures have been defined by SodM and Rijkswaterstaat Data-ICT Dienst (RWS-DID) in Januari 2008. In addition, in 2014 Industry guidelines have been defined, which have been published by "Technisch Platform Bodembeweging" (TPB) in a document titled "Geodetische basis voor Mijnbouw, Industrieleidraad, Versie 1.0", which is approved by SodM. The levelling networks are designed such that the benchmarks at the edges of the network are just outside the subsiding area.

Results of the surveys are officially reported in the Survey Register which is publically accessible. The Survey register consists of a free network adjustment (1st phase) as a quality control on the observations, a state of differences with relative heights (relative to the chosen reference benchmark) and height differences of the benchmarks between epochs, and a map of the survey network and benchmark locations, labelled with the height differences between the last and previous epoch. The reported height differences are not corrected for possible autonomous movement but present the total displacement at surface. The interpretation of the root cause (be it deformation due to gas extraction, autonomous movement or otherwise) can only be carried out by expert analysis and is not part of the survey register.

6.3.2 Surveying techniques

Current surveying techniques are:

- Spirit levelling
- PS-InSAR (Satellite Radar Interferometry)
- GPS (as part of GNSS: Global Navigation Satellite System)

6.3.2.1 Spirit Levelling

This technique has been used for Groningen since 1964.

Surveys are executed according to regulations defined by RWS-DID as stated in 'Productspecificaties Beheer NAP, Secundaire waterpassingen t.b.v. de bijhouding van het NAP, versie 1.1 van januari 2008'.

The equipment used includes certified, self-registering, optical levelling instruments and barcode level staffs. Measurements are registered fully automatic in a registration and validation system defined by RWS-DID.

6.3.2.2 PS-InSAR

Since 2010, deformation based on PS-InSAR technique is reported, in conjunction with a number of levelling trajectories for validation.

Deformation is estimated from phase differences between the acquisitions and persistent scatterers (Hanssen, 2001). The spatial resolution depends on the presence of natural reflectors, such as buildings. To obtain a precision comparable to levelling, error sources (like atmospheric disturbance, orbital inaccuracies) need to be estimated and removed. To support this, a time series of satellite images is required (>20-25 images) and ample resolution of scatterers. The estimated deformation velocity from InSAR observations is 0.5-2 mm/year (see Ketelaar, 2009).

The big advantages of the InSAR technique are its high temporal resolution (> 10x per year) and the dense spatial resolution. No survey crew is required in the field, hence no disturbance of the area and no security risks. Moreover, the accuracy of PS-InSAR is comparable to levelling.

6.3.2.3 GPS

Global Positioning System (GPS) stations have been placed at 10 Groningen field facilities; Eemskanaal; Froombosch, 't Zandt, Overschild, Tjuchem, Tankerpark Delfzijl, Zuiderveen, Stedum, Usquert and Zeerijp. A first GPS station was already placed on the Ten Post location in Q1 2013. The new stations are recording since 26th March 2014. GPS stations are continuously monitoring the horizontal and vertical components of subsidence of the ground surface. They are best placed on an existing building. Locations Stedum, Usquert and Zeerijp, do not have buildings. There, a three legged reinforced concrete construction was placed to anchor the GPS. Data is transferred from the GPS locations by 3/4G modems.

6.3.3 Survey design

6.3.3.1 Levelling network

The Groningen levelling network is part of the bigger Northern Netherlands network. Figure 6-2 below displays the levelling network, as surveyed in 2013.

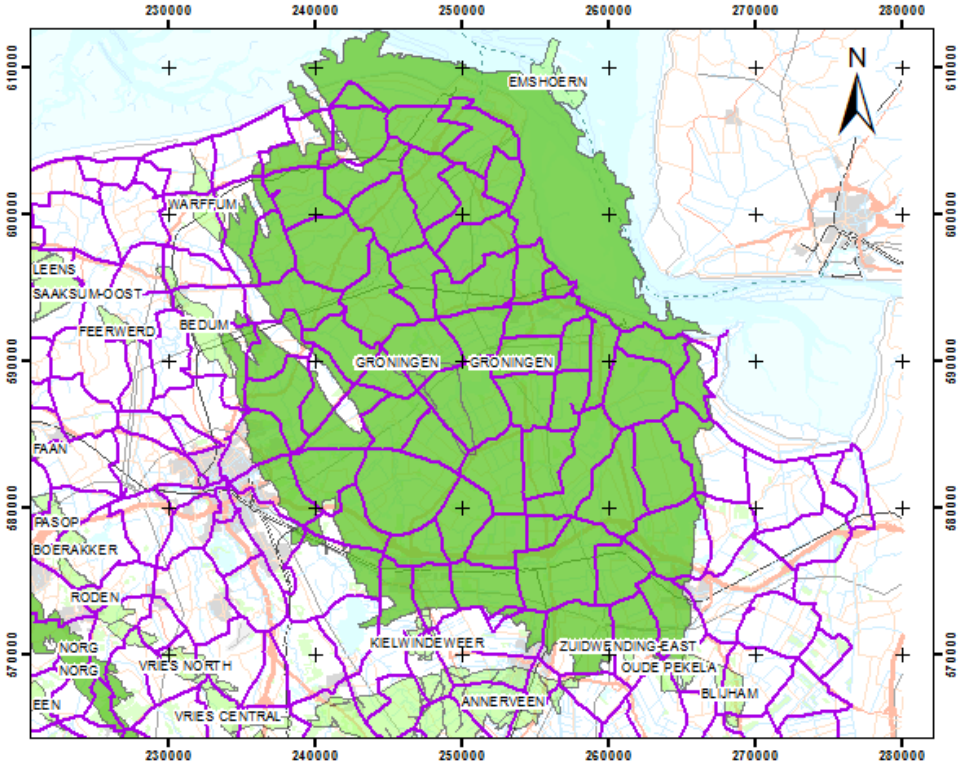

Figure 6-2 Levelling network Groningen field

6.3.3.2 PS-InSAR

The persistent scatterers (PS) have a constant reflection in time and space and correspond merely with buildings in the terrain. Figure 6-3 below shows in green dots the persistent scatterers as detected in the descending Radarsat-2 track.

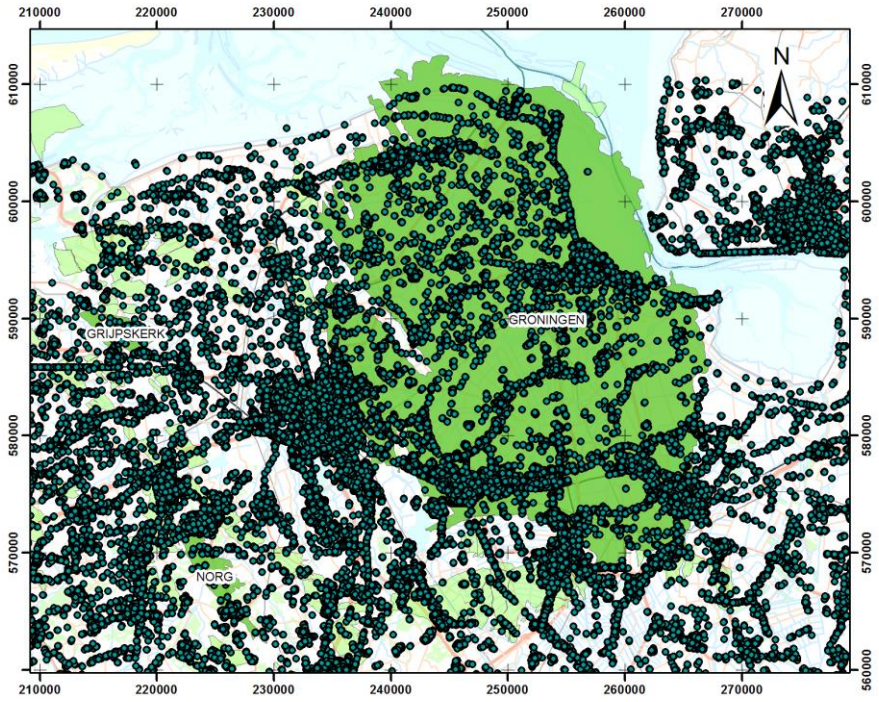

Figure 6-3 Spatial coverage with Persistent Scatterers in North-east Netherlands on the basis of images from descending Radarsat-2 track

6.3.3.3 GPS

The locations of the continuously recording GPS stations in the Groningen field are shown in Figure 6-4.

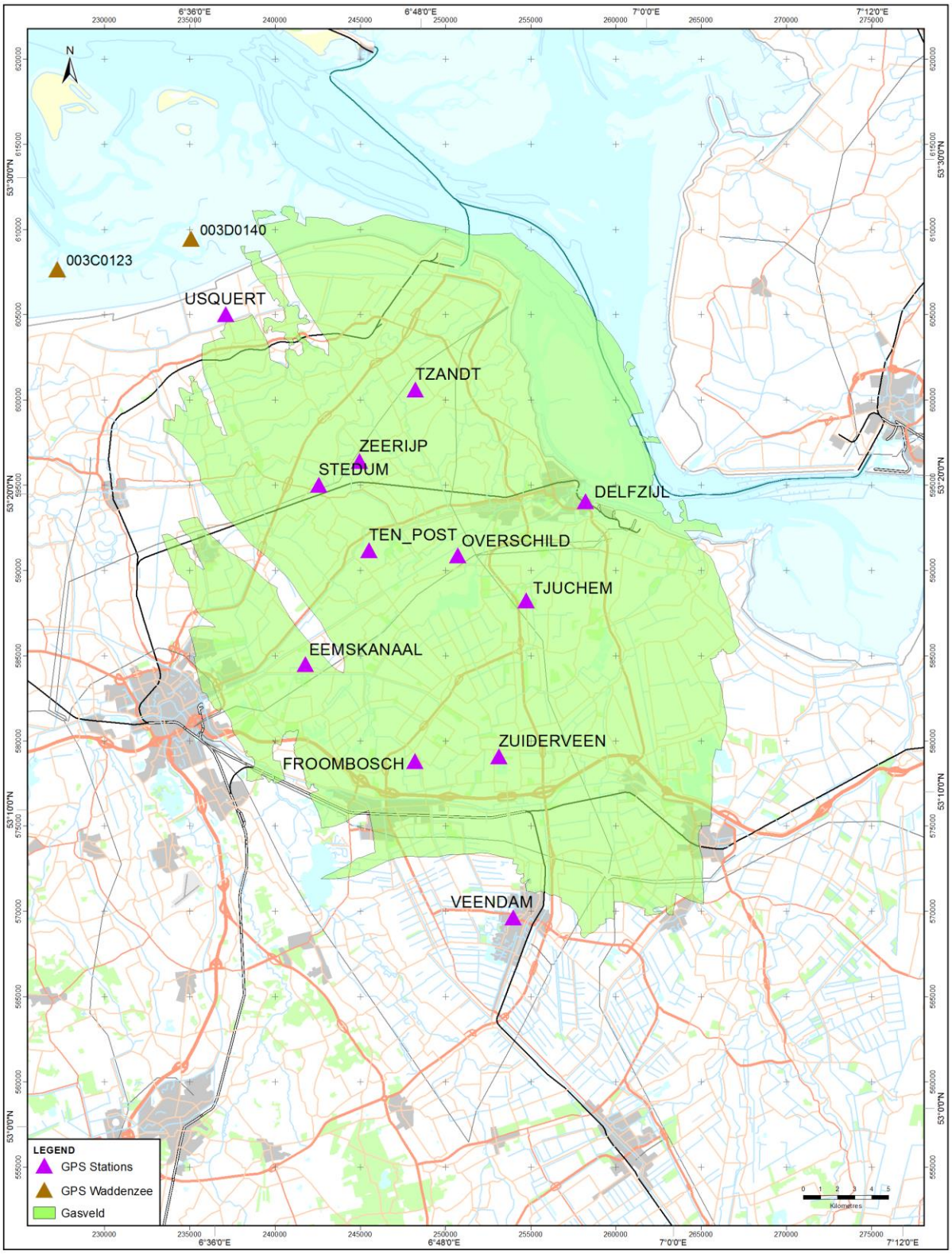

Figure 6-4 Location of the GPS stations in the Groningen field.

6.3.4 Levelling and InSAR data used for the calibration

The calibration is done on the "differentiestaten", a list of differential heights of the benchmarks between epochs of the levelling campaigns, using benchmark 000A2080 nearby Gasselte (Drenthe) as reference point.

The measured height differences of the levelling surveys are processed with the geodetic program Move3 in a free network adjustment.

The benchmarks within the area bounded by a purple square indicated in Figure 6-8 are used. RMS values were calculated for each benchmark as described in section 6.5.1. 8 out of 1000 benchmarks were excluded from the dataset as they were showing a very high RMS (higher than 7) value and showing a temporal subsidence pattern that is in disagreement with the subsidence behaviour observed in neighbouring points.

Two sets of levelling data have been used to calibrate the model. The first set only contains data that were recorded in the full levelling campaigns. These datasets are: H_15_04_1964, H_01_09_1972, H_01_09_1975, H_15_07_1978, H_01_07_1981, H_01_09_1985, H_01_08_1987, H_15_05_1990, H_14_05_1991, H_28_06_1993, H_13_06_1997, H_05_06_1998, H_17_06_2003, H_13_08_2008, H_25_04_2013,

Next to the levelling surveys also Insar surveys were used. Instead of using the Insar data as a separate dataset the Insar data were integrated with the levelling data (Figure 6-5). These combined datasets used in the calibration are: D_29_03_1993, D_30_03_1995, D_29_03_1996, D_29_03_1997, D_30_03_1998, D_30_03_1999, D_29_03_2000, D_29_03_2001, D_29_03_2004, D_29_03_2005, D_30_03_2006, D_30_03_2007, D_29_03_2008, D_29_03_2009, D_30_03_2010, D_30_03_2011, D_29_03_2012, D_29_03_2013, D_30_03_2014, D_30_03_2015.

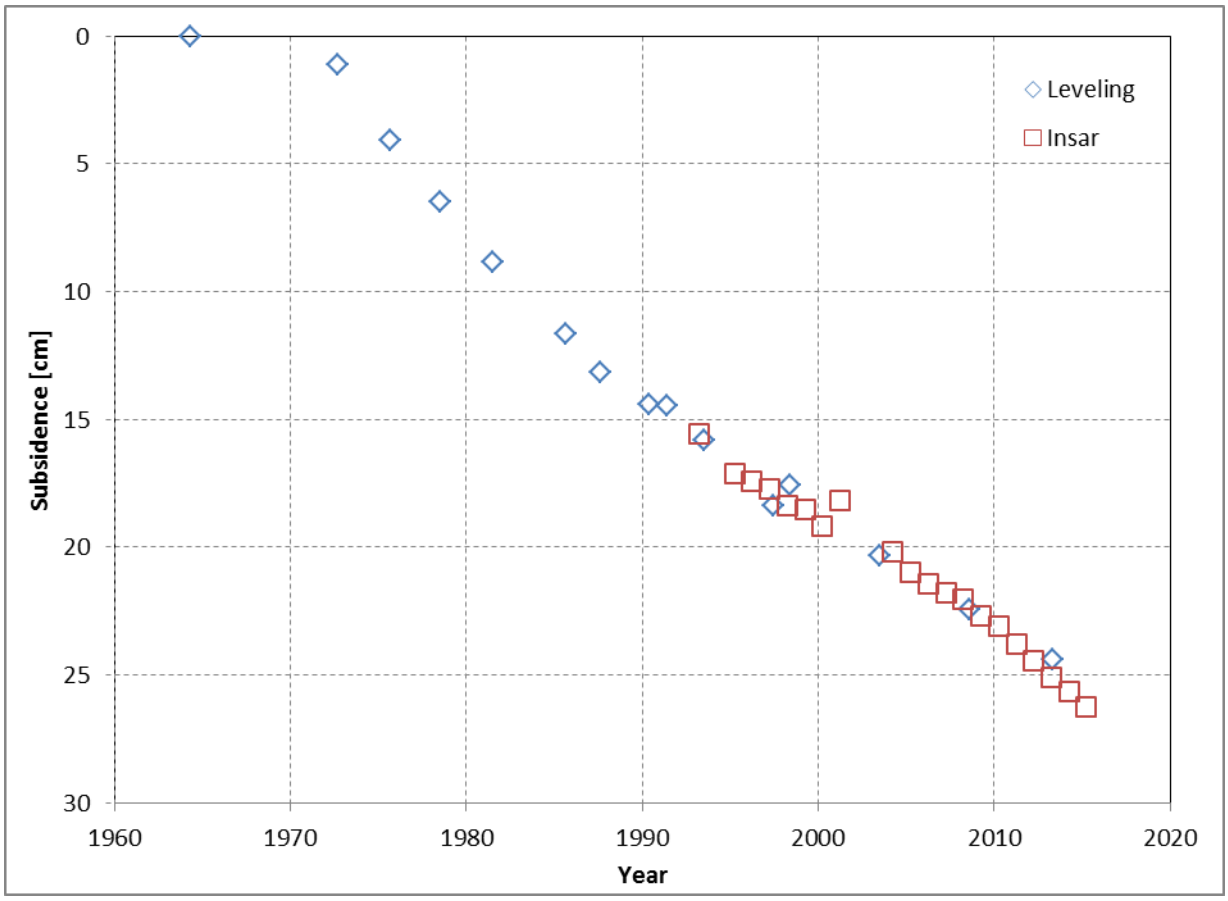

Figure 6-5 Integration of the Insar data (red squares) with the levelling data (blue diamonds)

6.3.5 Data from uniaxial compaction experiments

Subsidence measurements are the primary data source used that calibrate the geomechanical models. In addition, compaction experiments on plugs taken from reservoir core samples provide insight into the compressibility of the reservoir rock.

However, conclusions should be drawn with care. The sparse sampling density of core material cannot fully constrain the spatial variability of the reservoir compressibility. Similarly, the total compaction of the reservoir formation is a function of the reservoir thickness and the changes in pore fluid pressure and there are uncertainties, especially away from wells where this data has been measured. In recent years much

consideration has been given to the unloading of the core confining stress during exhumation, which can lead to the possible development of micro-cracks, thus making the samples more compressible. The expectation is that such 'softening' would be especially marked during the first cycle of a multi-cycle compression test. But there are many other sources of uncertainty. Therefore, the models should first match the subsidence data, while the reservoir compressibility should fall within the range of measured plug data.

6.3.5.1 Rotliegendes core samples

The Groningen Cm-values [*10^{-5}bar^{-1}] compare well with all other available data on Rotliegendes core plugs. Figure 6-6 plots these values as a function of porosity. A best-fit cubic polynomial trend line with porosity fraction [-], using a least-squared regression based on all data (L2 norm), is also plotted in the graph. Based on the good agreement between Groningen data and the overall ROSL data, it was decided to use this regression fit as a starting point for the calibration of the geomechanical model to the subsidence measurements:

$$C_m = 267.3\phi^3 - 68.72\phi^2 + 9.85\phi + 0.21$$

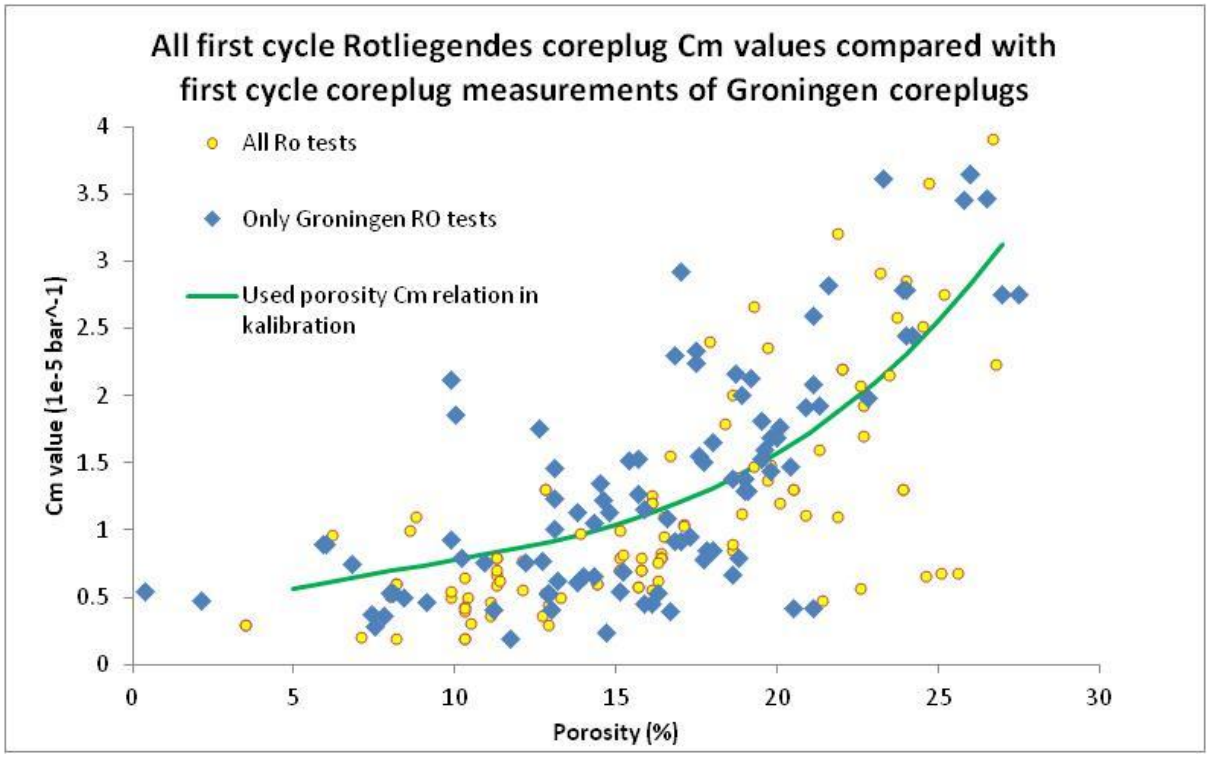

Figure 6-6 Comparison of the Groningen data to all available ROSL Cm values as a function of atmospheric porosity

6.4 The Groningen Geomechanical model

The Groningen geomechanical model computes the compaction due to depletion at reservoir level and transfers the derived strains to surface subsidence by using a semi-analytical approach (Geertsma 1973 and Geertsma and van Opstal, 1973). This methodology is incorporated in Shell's 'SubCal' software.

The compaction model has the same dimensions as the MoReS reservoir simulation model. The extent of this compaction model is shown in Figure 6-7. The areas in blue indicate the location of the aquifers. Compared to the 2013 winningsplan the MoReS simulation model has been extended. This has been done to explicitly model the aquifer depletion surrounding the Groningen field.

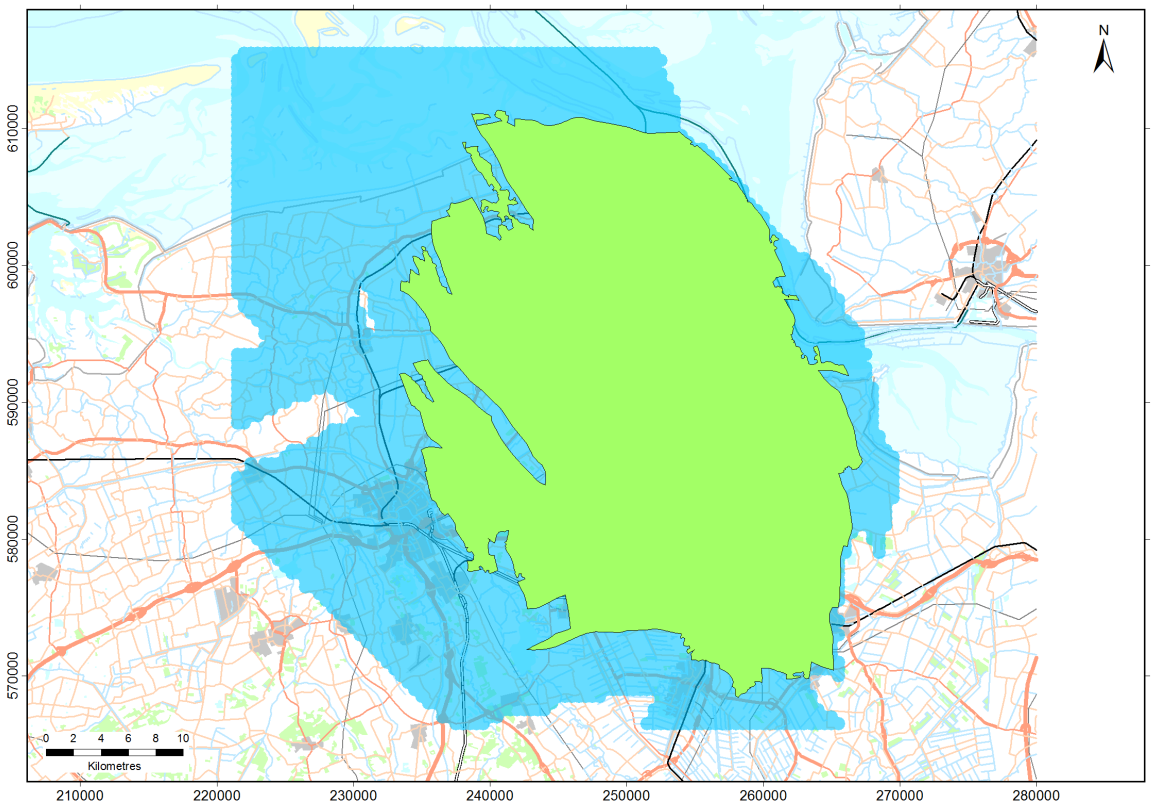

Figure 6-7 *Outline of the geomechanical model; green indicates the gas-bearing part, and blue the water-bearing part included in the Mores model.*

The geomechanical model uses the top reservoir map, the reservoir thickness, the reservoir pressure and the porosity as an input for the calculations. The model consists of one single reservoir layer instead of the 30 MoReS layers and therefore an upscaling method is applied that is documented in more detail in section 6.4.3.

When calibrating the model to the measured subsidence, the subsidence effect caused by neighboring fields is removed by making the area in which the benchmarks are chosen in the west and south smaller than the extent of the compaction model. In the south the area is further restricted because the subsidence in this area is affected as well by salt mining between Annerveen and Groningen (see Figure 6-8).

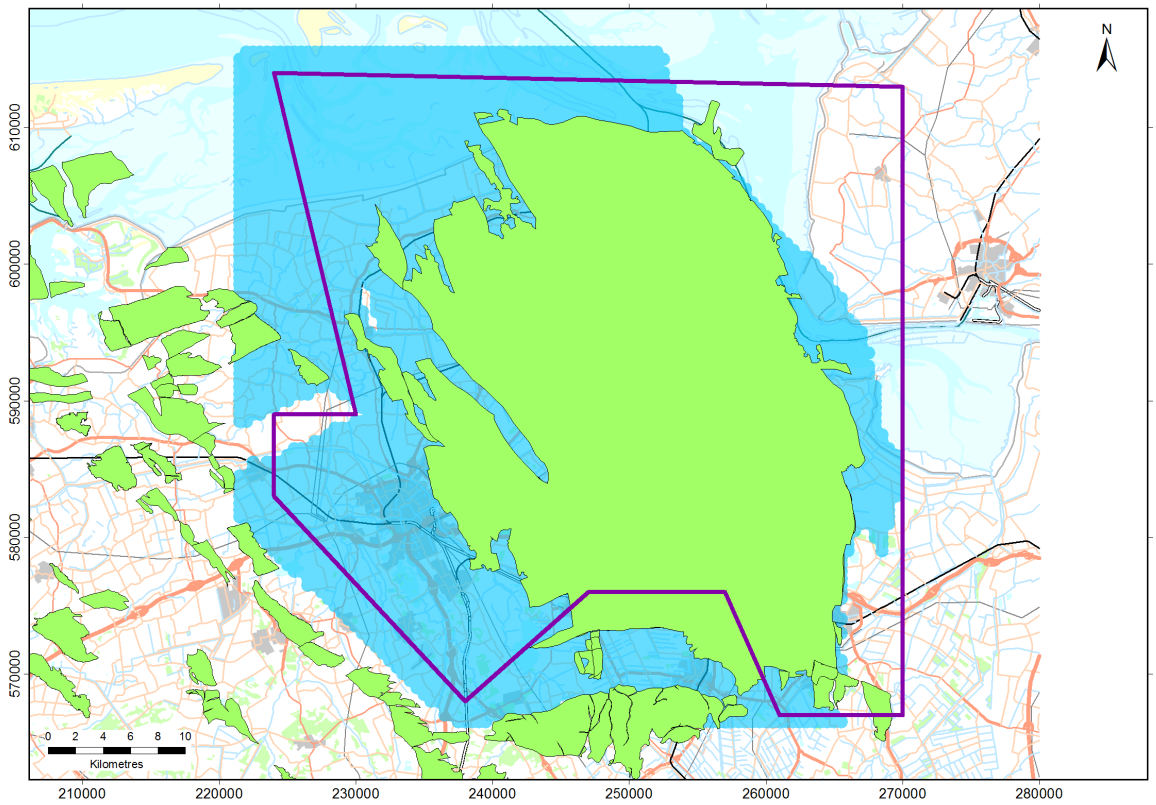

Figure 6-8 Area definition of the benchmarks used in the calibration (within the purple polygon).

The compaction at reservoir level is calculated with two different compaction models, the time-decay and the isotach model, which are both outlined in the next paragraphs. Calibration of the models to the subsidence data is described in section 6.5.

6.4.1 Time Decay Compaction model

The observation of a delayed, slowly accelerating subsidence at the onset of pressure depletion in combination with continuing subsidence after depletion has ceased, is consistent with a time lag (time decay) process where the subsidence response to reservoir compaction is asymptotic, with a characteristic time decay constant. Processes of this type are fundamental and commonplace throughout the natural world; they are the signature of non-equilibrium dynamical systems. The archetype of processes in this class is the familiar diffusion or heat equation. Time decay type models have been proposed as explanations for subsidence delay in the past. Houtenbos [pers. comm., 2006] proposed a simple empirical time decay relationship between 'subsidence volume' and the mass of gas produced. A number of issues in the physical reasoning led to a rejection of this proposal by NAM and SodM. It was observed at the time though, that transfer functions of this type did appear to provide a satisfactory temporal match to subsidence data and that they are characteristic of a diffusive, and therefore physically reasonable, process. A distantly related time dependent process was contained within the Rate Type Compaction Model [RTCM] (de Waal, 1986), which also sought to explain observed subsidence delay above a number of reservoirs.

6.4.1.1 Volumetric Time Decay

While it cannot be claimed that the precise cause of the volumetric time decay process has been identified, it seems highly likely that it is associated with volume strain in the reservoir rather than elsewhere in the subsurface. The constrained volume strain, e_{ii}, at a point, **x**, in the reservoir is then the usual instantaneous product of pressure change, Δp, and constrained uniaxial compressibility, c_m, but now convolved with a time decay function.

$$e_{ii}(\mathbf{x},t) = \Delta p(\mathbf{x},t)\; c_m(\mathbf{x})\; *_t \frac{1}{\tau}\exp\left[\frac{-t}{\tau}\right]$$

Here, t, is time, $*_t$, is the convolution operator with respect to time and, τ, is a time decay constant. The best fitting time decay constants for the Groningen field were found by inversion using a semi-analytic geomechanical model and have values of some 3 to 8 years.

It should be realised that it is quite possible that the observed time decay is not a material property of the reservoir rock, but could be due to particularities of the reservoir geometry, pore fluids or some other factor. Therefore it cannot be assumed that the time decay constant appropriate for one reservoir can be applied to another based simply on rock type.

6.4.2 Isotach formulation of the Rate Type Compaction model

In the Netherlands, a form of this model is the most accepted model for settlement calculations in soft soil. The model is also known as the a,b,c isotachen model (den Haan, 2003). TNO (2013) investigated the application of this model on cemented rock using the laboratory experiments from de Waal as a starting point (De Waal, 1986). Adjustments of this a, b, c isotachen model led to the definition of the isotach formulation of the rate type compaction model (RTCiM) which was also implemented by NAM and used to calibrate the compaction model and estimate future subsidence.
Figure 6-9 shows the Standard Linear Solid (SLS) model, the most simple form of the general isotach model, as a spring-dashpot system (TNO, 2013)

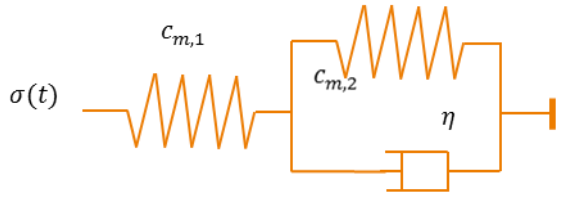

Figure 6-9 Representation of the SLS model

The compaction in the RTCiM model is calculated according the following numerical scheme The simulation is started from the state where effective stress σ' is equal to reference effective stress σ'_{ref}, and elastic strain is equal to the secular strain which are at start (t) zero $\varepsilon_d = \varepsilon_s = 0$, $t = 0$ and increases with a fixed time step size Δt. The effective stress as a function of time $\sigma'(t)$ is known as well as $\sigma'(0)$ which is given as $\sigma'(0) = \sigma'_{ref}$ as otherwise $\varepsilon_d \neq 0$ at $t = 0$. The compaction is calculated using the following algorithm:

1) Use current σ' and $\varepsilon = \varepsilon_d + \varepsilon_s$ and calculate secular strain rate $\dot{\varepsilon}_s$ from

$$\dot{\varepsilon}_s = \left(\frac{\varepsilon - \varepsilon_0}{\sigma'} - C_{m,a}\right)\dot{\sigma}'_{ref}\left(\frac{\varepsilon - \varepsilon_0}{\sigma' C_{m,ref}}\right)^{-1/b}$$

2) Calculate increase in secular strain $\Delta\varepsilon_s = \dot{\varepsilon}_s \Delta t$ and update ε_s

3) Update $t = t + \Delta t$

4) Calculate direct strain ε_d from $\varepsilon_d = C_{m,a}(\sigma' - \sigma'_{ref})$ using the new $\sigma'(t)$

5) Calculate $\varepsilon = \varepsilon_d + \varepsilon_s$

After step 5 the algorithm goes back to step 1.

6.4.3 Upscaling of input data

The reservoir modelling has been performed using Shell's reservoir simulator MoReS. It uses a 3-dimensional gridded reservoir structure, which includes porosity and permeability information and attempts to solve for the fluid flow and pressure changes as constrained by historic production and pressure data taken from wells. The reservoir model therefore contains self-consistent porosity and pressure change information that should be used in the geomechanical modeling. However, the reservoir model tends to use a finer grid size than is needed for the geomechanical model so 'upscaling' is required.

For the Groningen field, a MoReS reservoir model was built consisting of 30 vertically stacked layers and with grid dimensions of 250 m by 250 m, or less. The reservoir formation in the Geomechanical model is made up of

one single layer with a lateral element size of around 500 m by 500 m. It is therefore necessary to up-scale the MoRes parameters for the geomechanical model. This is achieved by post-processing of the MoRes output file using routines coded in the general purpose mathematics package, Scilab. Figure 6-10 shows an example of a MoReS output file. The files contain the grid pressures for a single time step and a separate file is generated for each time step.

Table 'Grdcentr' contents; generated on Thu 04/03/2010 16:21 from run '001_BMBoxBehnken_two_200x200_001p

	date	xcentr	ycentr	zcentr	dikte	la	Pgrid	net_gross	porosity
	YEAR	M	M	M	M	INTUNIT	BAR	REALUNIT	REALUNIT
1	2036.997	206460	601770	-4249.4	1.0245	1	502.6	0.95535	0.09637
2	2036.997	206650	601770	-4221.5	1.0273	1	499.99	0.96162	0.093082
3	2036.997	206850	601800	-4195.3	1.0332	1	496.85	0.9582	0.14334
4	2036.997	207040	601850	-4174.8	1.0419	1	494.81	0.96528	0.12991
5	2036.997	207230	601900	-4160.2	1.051	1	493.52	0.94872	0.11788
6	2036.997	207410	601940	-4148.3	1.0601	1	492.16	0.94102	0.1321

Figure 6-10 Example of a Mores output file, la indicates the layer number.

Upscaling of the reservoir pressure has to take into account the variability in the porosity and pressure depletion between the vertically stacked reservoir layers, and weigh them accordingly. This is achieved by summation of the reservoir layer compaction as a function of the layer pressure depletion and compressibility, the latter being a function of porosity. This upscaled compaction has to be equal to the compaction derived for the upscaled layer. The porosity of this upscaled layer is:

$$\emptyset_{\mathrm{av}} = \frac{\sum_{\mathrm{i}}(\mathrm{h}_{\mathrm{i}}\emptyset_i)}{\sum_{\mathrm{i}} h_i}$$

Where $\emptyset_i$ and h_i are the porosity and thickness for each reservoir model layer, respectively. Summation is over the appropriate number of grid layers.

Upscaling the pressure change is less straightforward. The objective is that the up-scaled compaction using a Δp_{avg} is the same as the compaction from the non up-scaled model. The effect of compaction in the individual layers should therefore be included in the upscaling procedure.

The change in thickness of each reservoir model layer is given by:

$$\Delta h_i = c_m(\emptyset_i)\Delta p_i h_i$$

Where $c_m(\emptyset_i)$ is the compaction coefficient as a function of the layer porosity and Δp_i is the pressure change in layer, *i*. The aggregate change in reservoir thickness across the vertically stacked layers is given by:

$$\Delta H = \sum_i c_{mi}(\emptyset_i)\Delta p_i h_i$$

where *H* indicates the stacked layer thickness. The upscaled pressure across the stacked thickness, $\overline{\Delta p}$, is then given by:

$$\overline{\Delta p} = \frac{\Delta H}{c_m(\emptyset_{\mathrm{av}}) * H}$$

This upscaled pressure was found to be insensitive to the detailed functional form of the compressibility-porosity relationship.

6.5 Calibration of the geomechanical model with geodetic data

For the purposes of subsidence prediction and preparation of the Winningsplan a representative, or 'base case', model must be selected. Throughout this document there are references to improved model fits and matches to subsidence data. This section describes the method used to make these judgments and the results for the different compaction models.

6.5.1 RMS of all benchmarks using epoch combinations

A relatively simple comparative measure of model fit was created by determining the residuals between the surveyed and modelled subsidence at all benchmarks for a number of different time spans, termed epochs, and calculating the total variance weighted root-mean-squared (RMS) value. A trivial sequential set of epochs can be envisaged, shown schematically in Figure 6-11(a), where the last survey of a previous epoch becomes the first survey of the next epoch. However, the comparatively small subsidence signal between subsequent levelling campaigns means that this approach would suffer from low signal-to-noise ratio. A comprehensive scheme including all possible epoch combinations could also be considered. Figure 6-11(b) schematically represents all the epoch combinations that include the first levelling campaign and similar epoch sets can be generated for each campaign, while excluding duplicates. This again though includes a large number of epochs with low signal-to-noise ratio while being considerably more computationally expensive. Instead a robust metric was created using a standardised subset of epochs that were of sufficient duration to provide good signal-to-noise ratio while keeping computation to a moderate level. These are shown schematically in Figure 6-11(c).

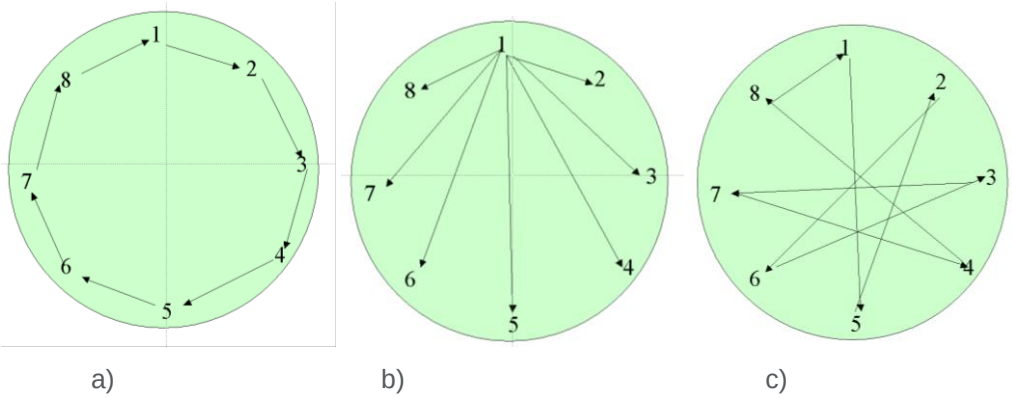

Figure 6-11 Schematic showing epoch combinations used in the calibration process: a) sequential, b) all possible combinations (example shows combinations with survey 1 only) c) efficient method used in current analysis.

Figure 6-12 shows an example plot where measured and modelled subsidence are plotted against each other for a variety of epochs from which the RMS value is calculated.

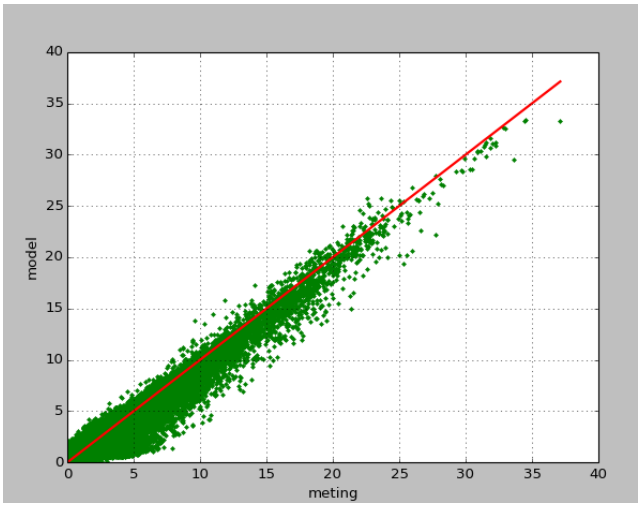

Figure 6-12 Example of an 'RMS' graph showing modelled against measured subsidence, in cm.

6.5.2 Winningsplan 2013 spatial fit

In the Winningsplan 2013 the compaction was based on a porosity-Cm relation, which implies that the subsidence will be biased by a (non-unique) porosity distribution based on expert judgment by the geologist. This method showed an under prediction of the subsidence in the south of the field while the model over predicted the measured subsidence in the north (Figure 6-13). This questions the use of such strict coupling between the porosity and the compressibility of the rock. The large scatter in the laboratory measurements as pointed out in Figure 6-6 further supports this.

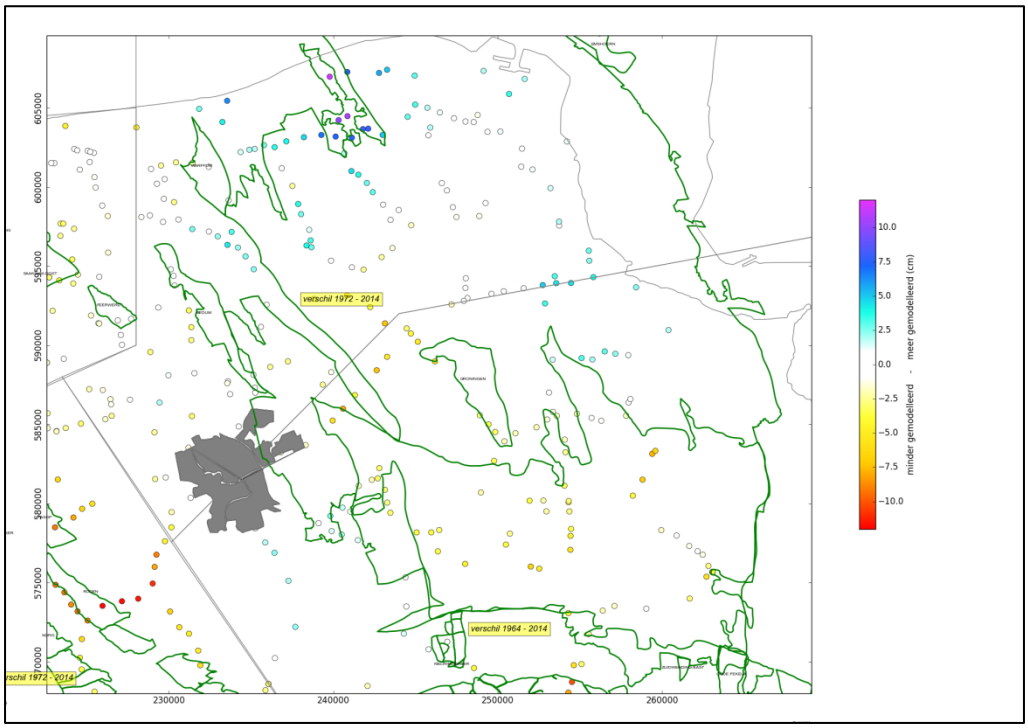

Figure 6-13 Difference between measured and modelled subsidence since start production for the Winningplan 2013 model.

In the current Winningsplan 2016 the spatial subsidence fit was improved by inverting to a spatially varying Cm grid with a grid size of 1x1 km^2. However inverting to the Cm value does not give a unique solution and can return large spatial scattering of the Cm. To reduce this scatter the inversion was regularized by using the Cm porosity relation (used in the Winningsplan 2013) as a prior. In the inversion process penalties were put on:

1. The difference between the inverted Cm and porosity derived Cm
2. The residuals between modelled and measured subsidence.

This resulting Cm grid is shown in Figure 6-14 and has been used for both the time decay and RTCiM model. In Figure 6-15 both the laboratory measured and the inverted Cm values are shown as function of porosity. To obtain an optimal subsidence fit in time for the different compaction models a multiplication factor was applied to the Cm grid obtained from the inversion.

In the next paragraphs the results are discussed in more detail for the various compaction models.

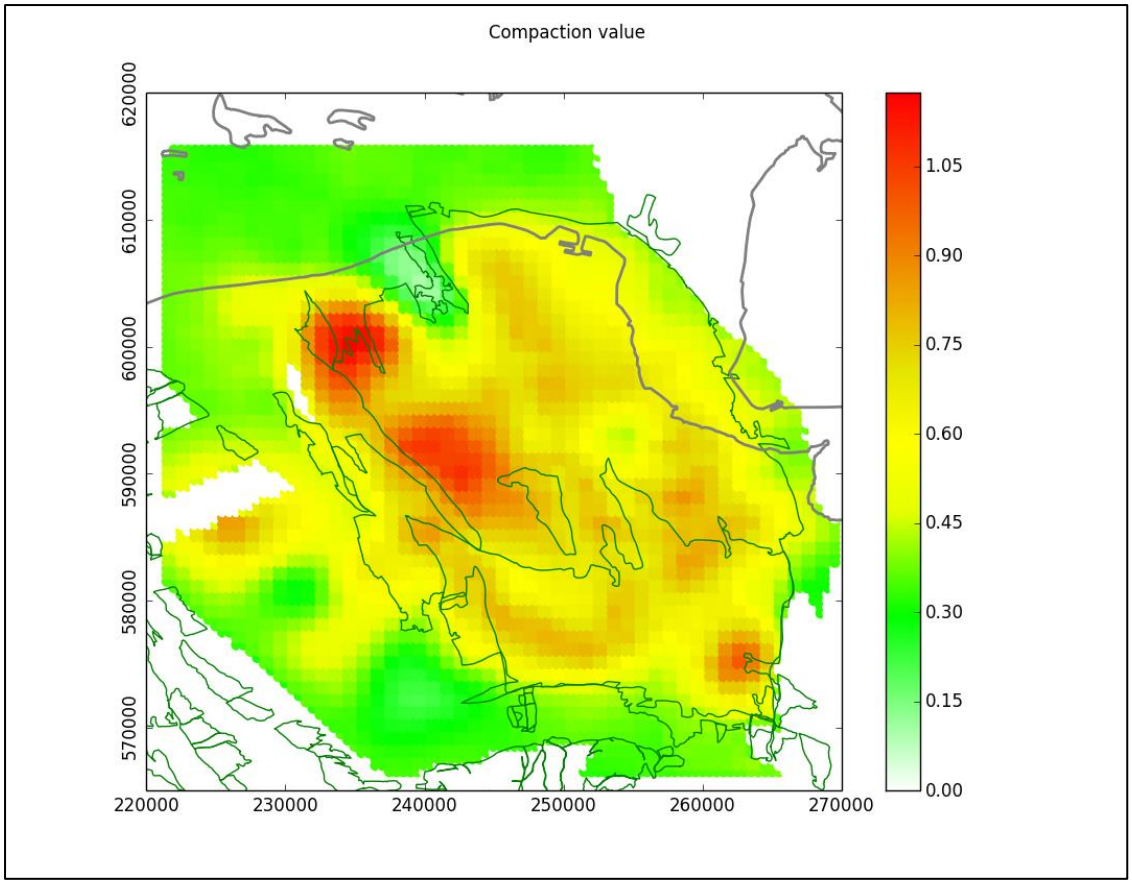

Figure 6-14 Cm (10^{-5}bar^{-1}) for Groningen calculated from inversion to subsidence*

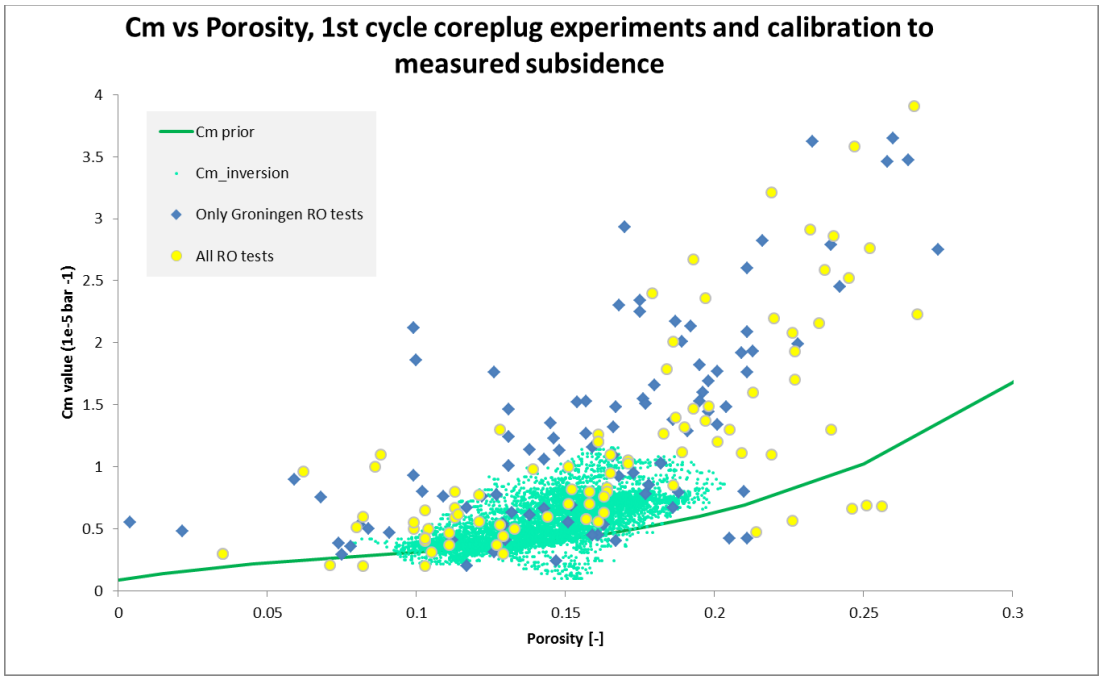

Figure 6-15 Cm porosity plot including the inverted Cm values for the Time decay model

6.5.3 Time Decay model

The calibration of the time decay model resulted in the following parameters for the time decay compaction model:

Cm multiplication factor is 0.94

decay time τ: 3 year

The difference between the measured and modelled subsidence between first and last measurement (2013) is shown in Figure 6-16. Note that the subsidence calculation has been done only for Groningen, other fields were not included in this calculation and therefore the difference between modeled and measured subsidence is increasing near the neighboring fields. The figure shows that the values for the residuals between model and observed data are very low.

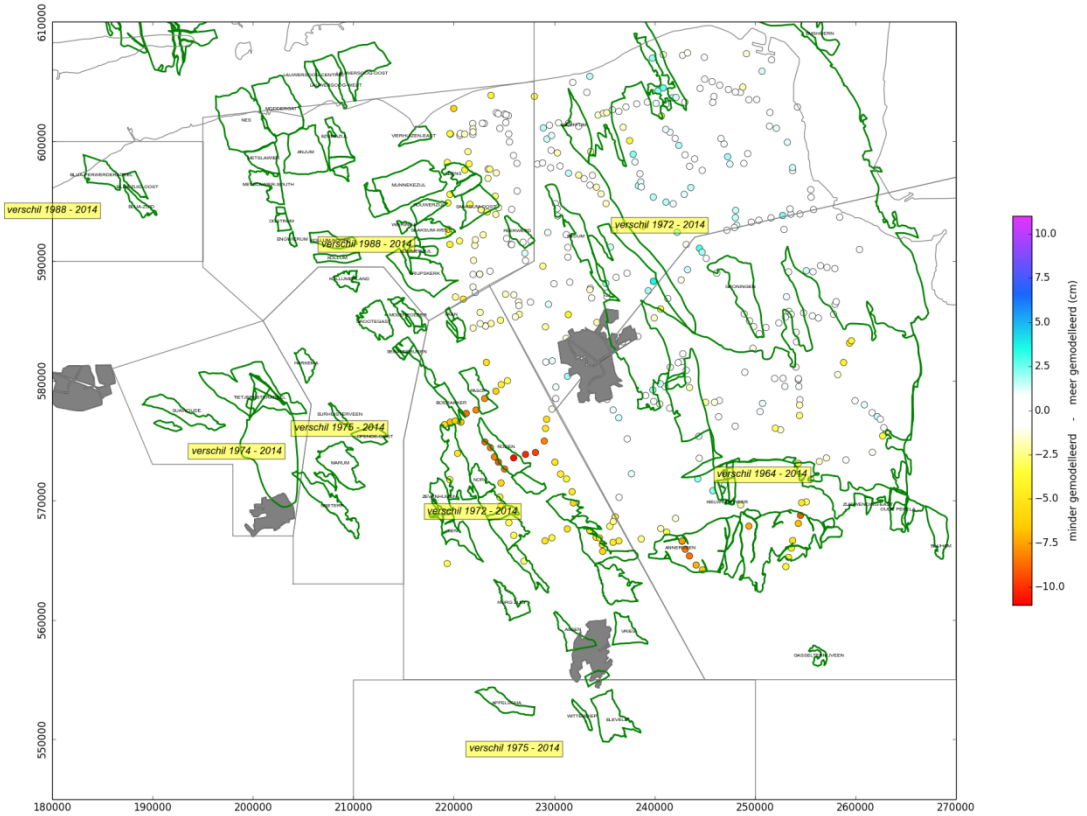

Figure 6-16 Time decay model: Difference between measured and modelled subsidence from start production/ first measurement until end 2013.

To investigate the uniqueness of the time decay parameters, a Monte Carlo simulation was carried out. The results of this analysis are shown in Figure 6-17. In this figure, the Cm multiplication factors are plotted against the decay times (in years) and the colors indicate the RMS value. This figure show a narrow bandwidth for the Cm but a wider bandwidth for the decay time τ.

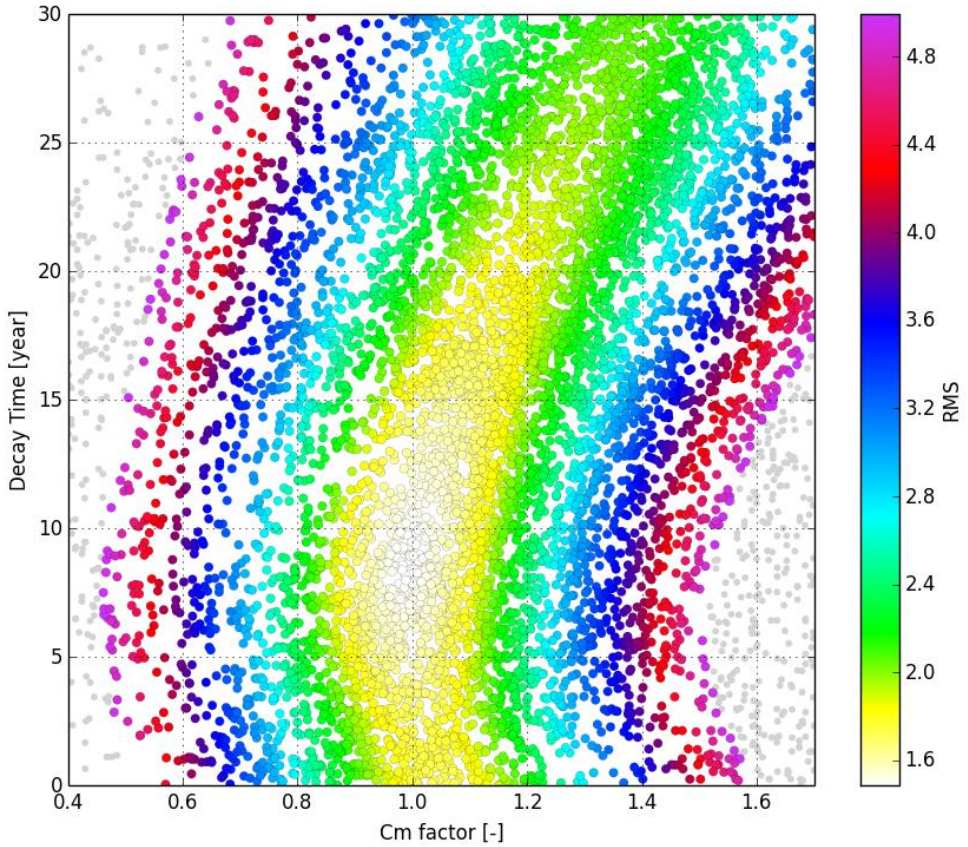

Figure 6-17 Monte Carlo analysis for the time decay model.

6.5.3.1 Conclusion

With a limited set of parameters that could be reasonably well constrained, the time decay model is able to produce a reasonable match with the observed data.

6.5.4 RTCiM model

The calibration to the RTCiM model resulted in the following parameters, $C_{m,ref}$ multiplication factor = 1.39, $C_{m,a}$ multiplication factor = 0.75, b = 0.018 and the $\dot{\sigma}'_{ref}$= 3.16 10^{-4} bar/year.

The $C_{m,ref}$ factor of 1.39 means that the Cm grid found by the inversion to the lateral Cm grid (Figure 6-14) is multiplied with 1.39. Comparing this resulting Cm grid with the coreplug measurements shows a good match with the first cycle Cm coreplug measurements (Figure 6-18)

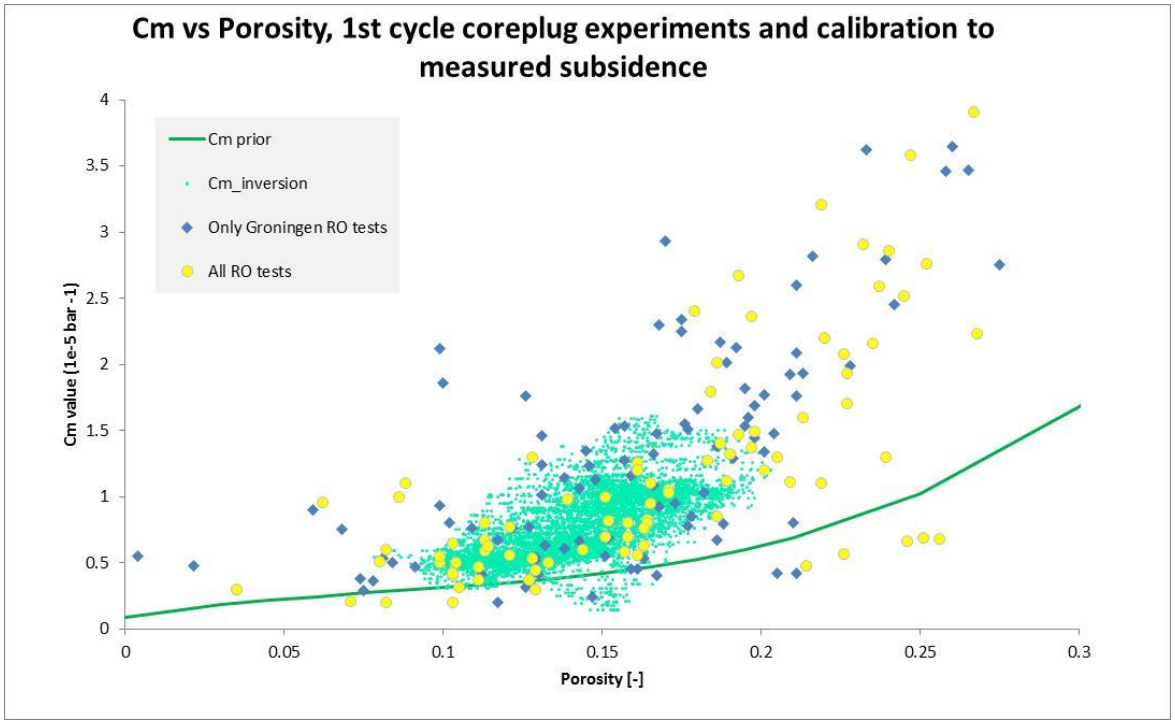

Figure 6-18 Core plug and inverted Cm for the RTCiM model

The spatial fit of this model is shown in Figure 6-19, in this plot the difference between modelled and measured subsidence is shown for the period 1972 – 2013. The figure shows that the values for the residuals between model and observed data are very low.

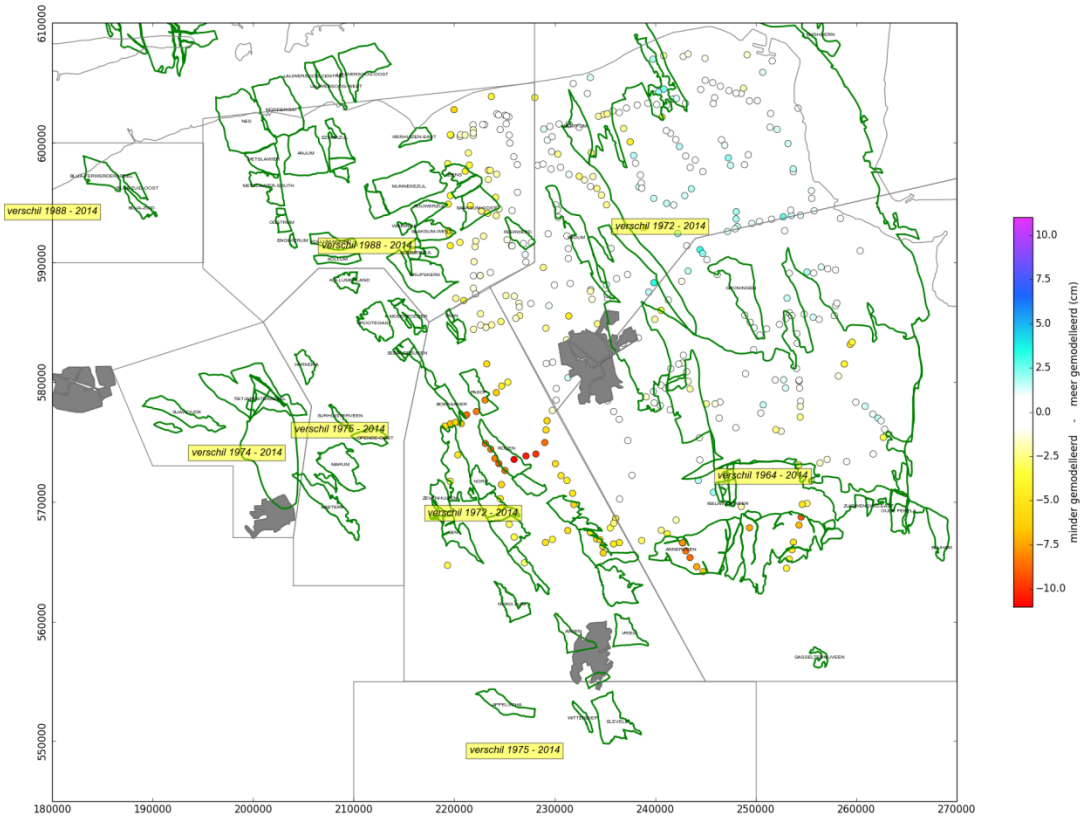

Figure 6-19 RTCiM: Difference between measured and modelled subsidence from start production/ first measurement until end 2013

The RTCiM model, as described in section 6.4.2, has three parameters. The uniqueness of possible parameter combinations has been investigated with a Monte Carlo simulation. The results are shown in Figure 6-20. The top row of these figures shows the RMS value against the various RTCiM parameters This figure shows that the three available parameters are reasonably well constrained. The $C_{m,a}$ and b are most constrained, but the $C_{m,ref}$ has a wider range. The bottom two graphs show a combination of two of the parameters. The colors in these figures indicate the RMS values.

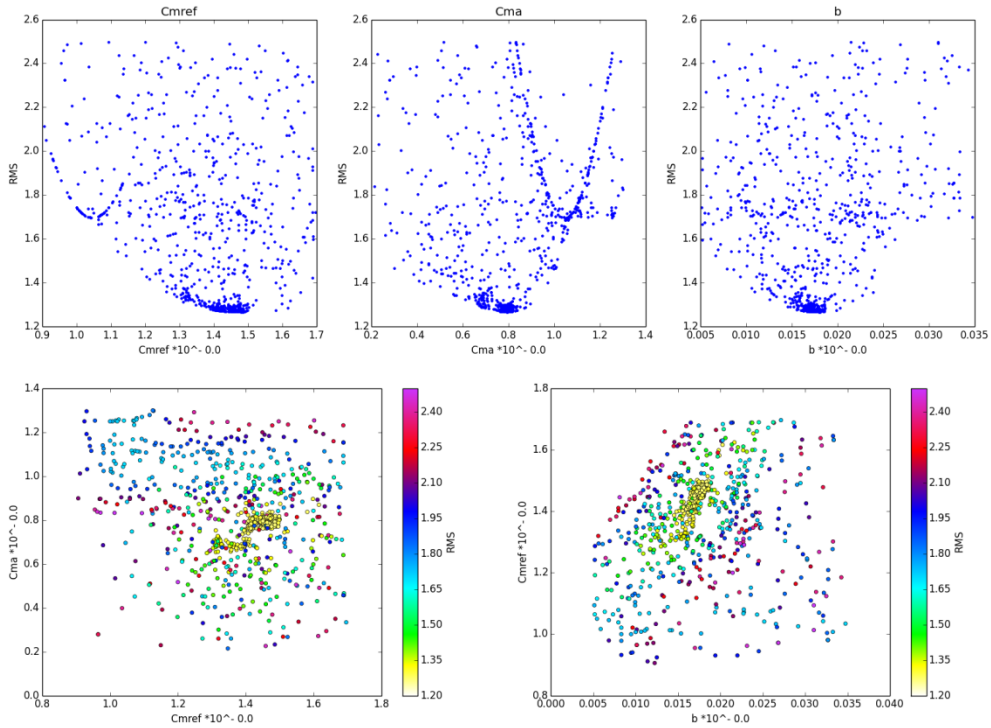

Figure 6-20 *Monte Carlo analysis for the RTCiM compaction model. The top row shows the different RTCiM parameters vs the RMS and the bottom row shows a combination of two parameters color-coded by the RMS value*

6.5.5 Comparison

As shown in previous paragraphs both compaction models show a good agreement with the measured subsidence after calibration. This is again demonstrated in Figure 6-21 for various benchmark locations.

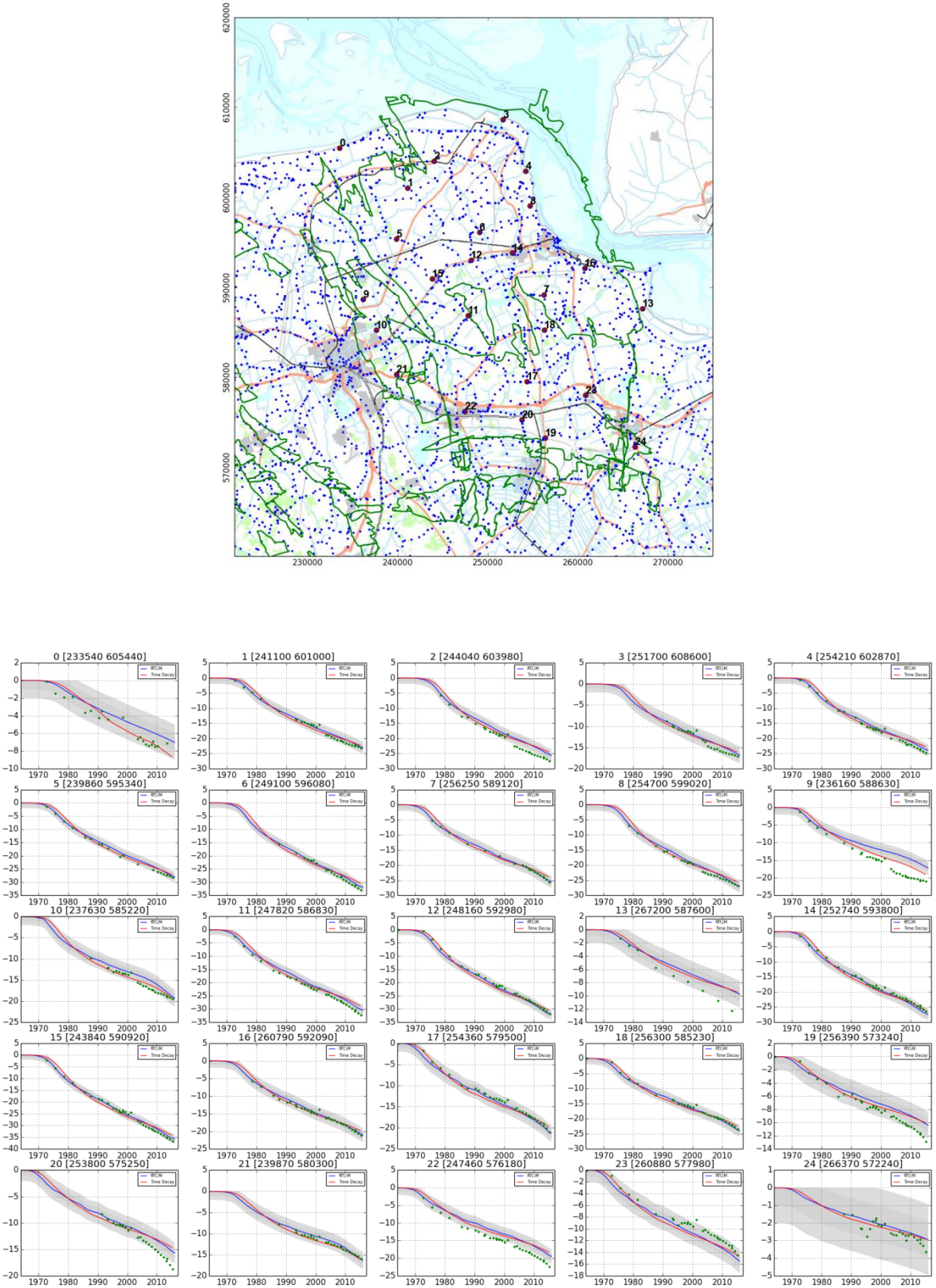

Figure 6-21 Comparison of the results from the Time decay and RTCiM models at the benchmark locations shown in the map. Note that the benchmark used in previous winningsplan 7E0033 is here point 12

6.6 RTCiM and Time Decay response to changes in production

To mitigate seismicity the gas production of Groningen was restricted. Noticeably the volumes of the production clusters in the north of the field were lowered. This resulted in a spatial redistribution of the production and depletion. The effect on subsidence is shown in Figure 6-22. The top row shows the subsidence at benchmark locations (using InSAR interpolation) for the period before (2010 -2012) and after (2013 – 2015) the production change. It can be observed that the higher subsidence values shifted to the south of the field. Note that the change in the subsidence pattern is about 5 mm, which is about the noise level.

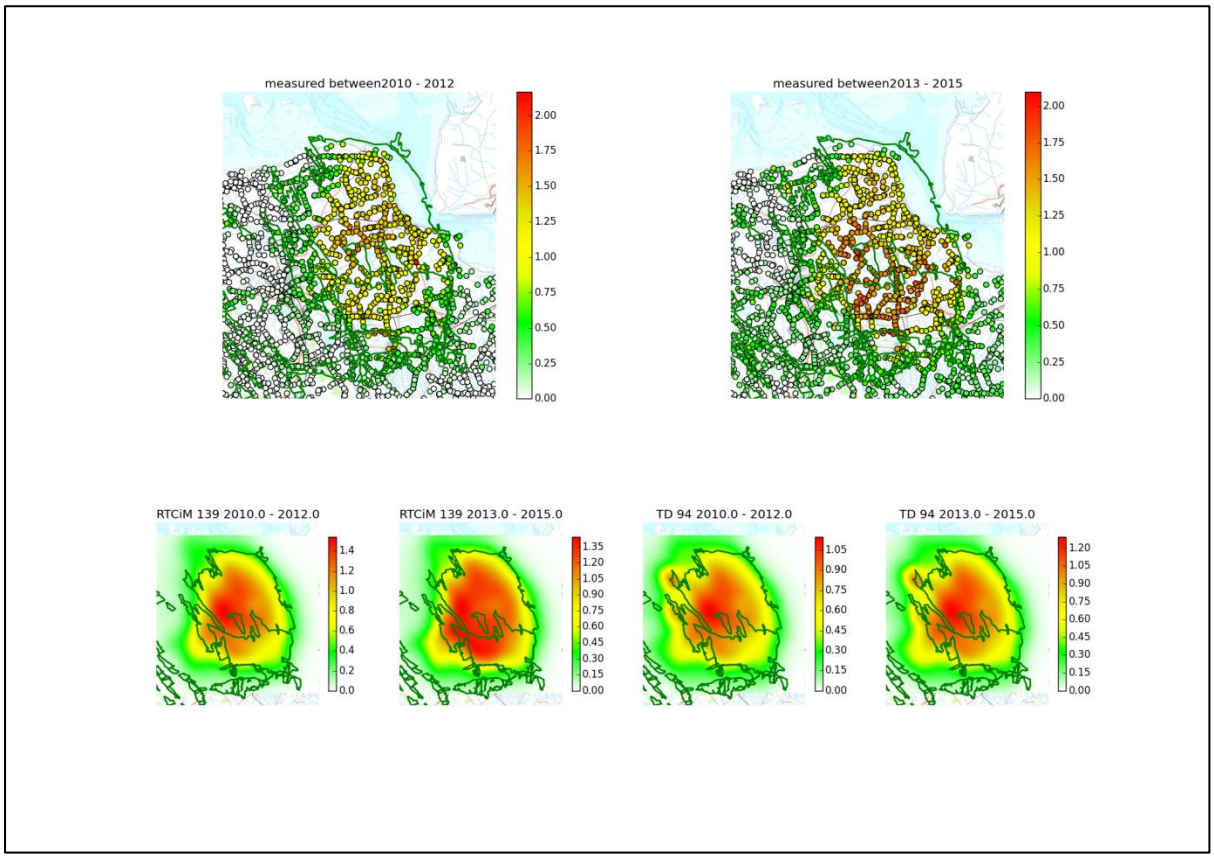

Figure 6-22 Change in subsidence pattern before and after the production change in 2013. Top row: measured subsidence. Bottom row: comparison between time decay and RTCiM model results (Subsidence in cm).

The bottom row shows the subsidence realizations for the RTCiM and time decay model for the same periods of time. The observed shift of the subsidence pattern to the south is reproduced best with the RTCiM model. Note that the RTCiM model does not cover the Bedum field in the North West, which shows about 1 cm of subsidence in the time decay model.

6.6.1 Selection of base case compaction model

Both the Time decay and the RTCiM compaction models result in a good overall fit to the observed subsidence data above the Groningen field.

The RTCiM compaction model is chosen as the base case compaction model because it results in the best fit to the temporal and spatial observed response of the subsidence to production changes.

6.7 Subsidence forecasts

As discussed above, two different compaction models were used for history matching and forecasting of subsidence with ongoing production. The RTCiM model was chosen as the base case model. In Section 6.5 it was shown that the two compaction models result in similar values for the subsidence at a point near the centre of the subsidence bowl.

The modelled base case (RTCiM) subsidence and the measured subsidence for the year 2013 are compared in Figure 6-23. Overall, the match with the observed measurements is reasonable to good. Figure 6-24 shows the forecast of the ultimate subsidence (status in 2100, approximately 30 years after the end of production) using the base case model. A maximum subsidence of some 50 cm is forecasted with this model.

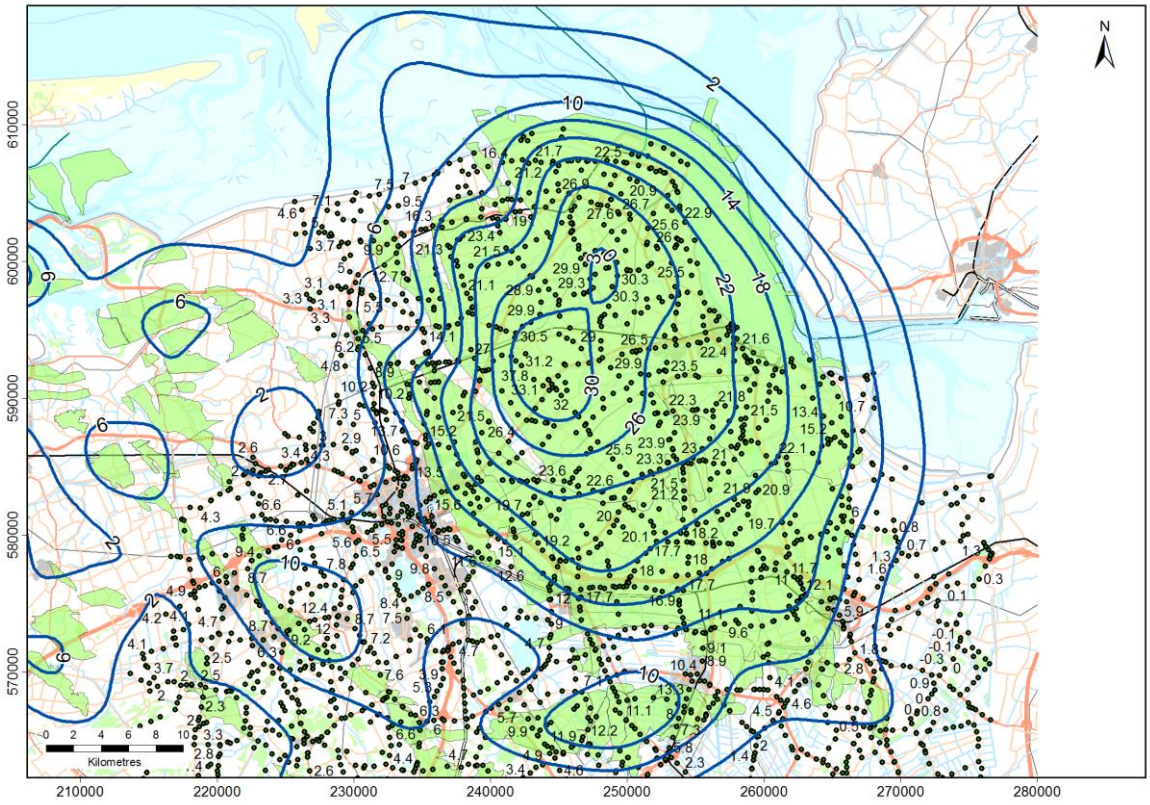

Figure 6-23 Measured subsidence at benchmarks vs modelled subsidence based on the RTCiM model (1972 – 2013, contours).

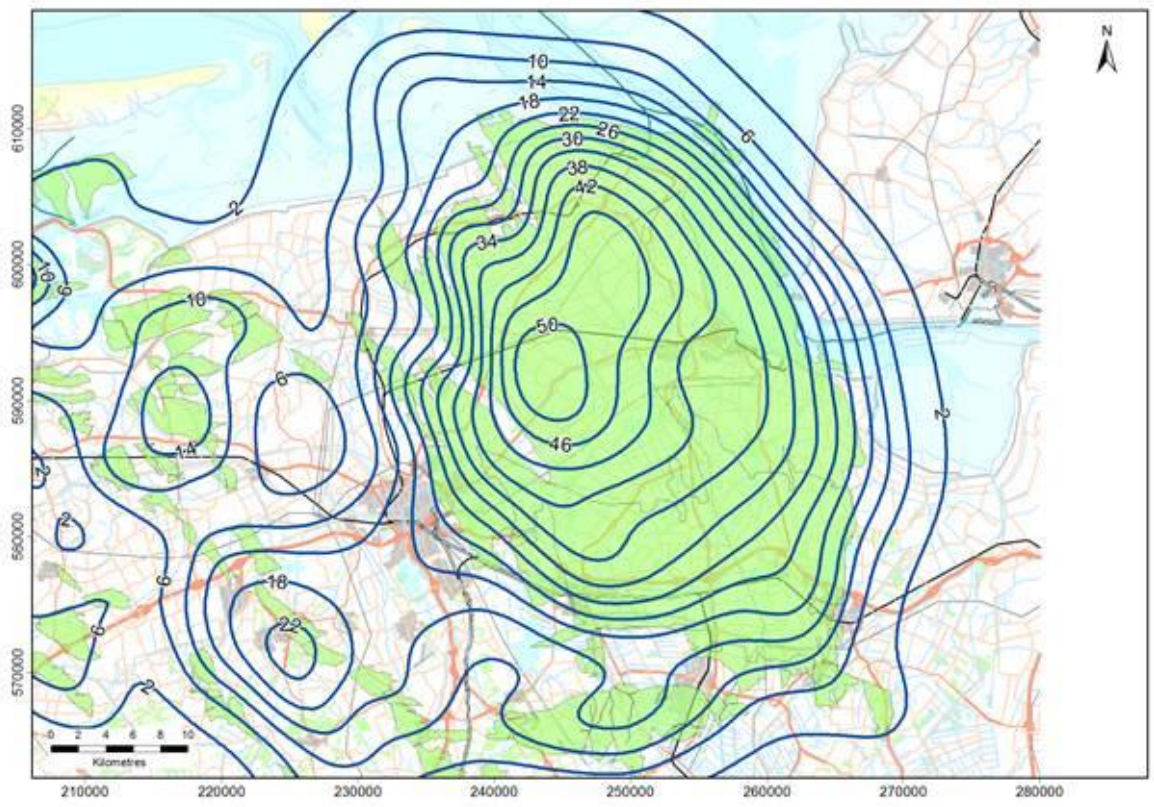

Figure 6-24 Subsidence prognosis based on the RTCiM model in 2100, approximately 30 years after the end of gas production. This figure shows the subsidence due to gas production for the Groningen field in combination with the subsidence predicted for other fields (subsidence in cm).

The development of the future subsidence through time for the different compaction models and different (optimized) gas production scenarios is shown in Figure 6-25 to Figure 6-28.

The RTCiM model reacts faster to changes in reservoir pressure than the time decay model. The Cm is also somewhat higher which leads to higher subsidence values. Compared to the "Statusreport 2015 (NAM, 2015)", in which the time decay model was used as the base case, the RTCiM model predicts an additional 4 cm subsidence in the deepest point at end of field life.

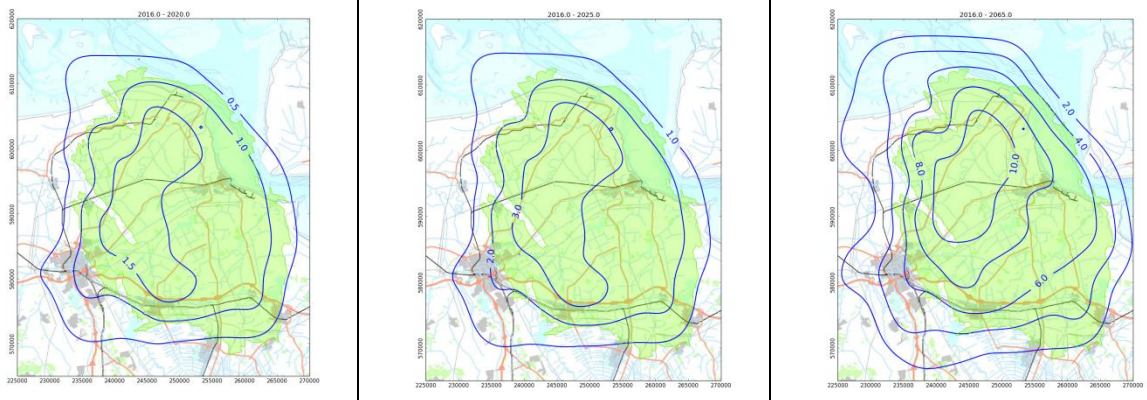

2016-2020	2016-2025	2016-2065

Figure 6-25 Development of future subsidence according to the time decay compaction model with 27 BCM annual production

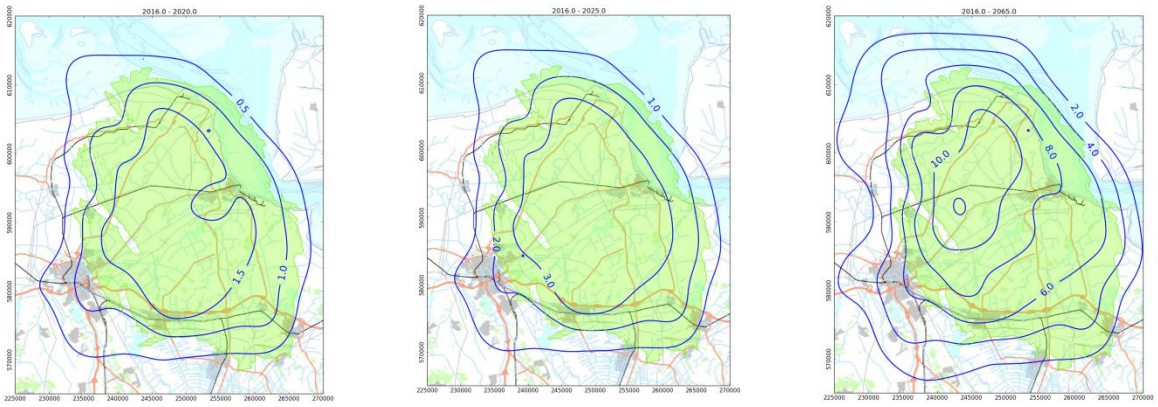

2016-2020	2016-2025	2016-2065

Figure 6-26 Development of future subsidence according to the time decay compaction model with 33 BCM annual production

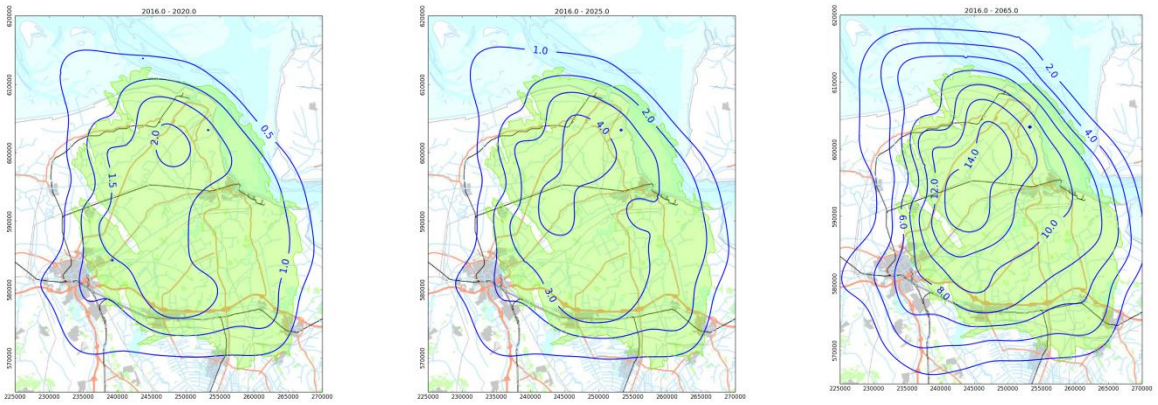

2016-2020	2016-2025	2016-2065

Figure 6-27 Development of future subsidence according to the RTCiM model with 27 BCM annual production

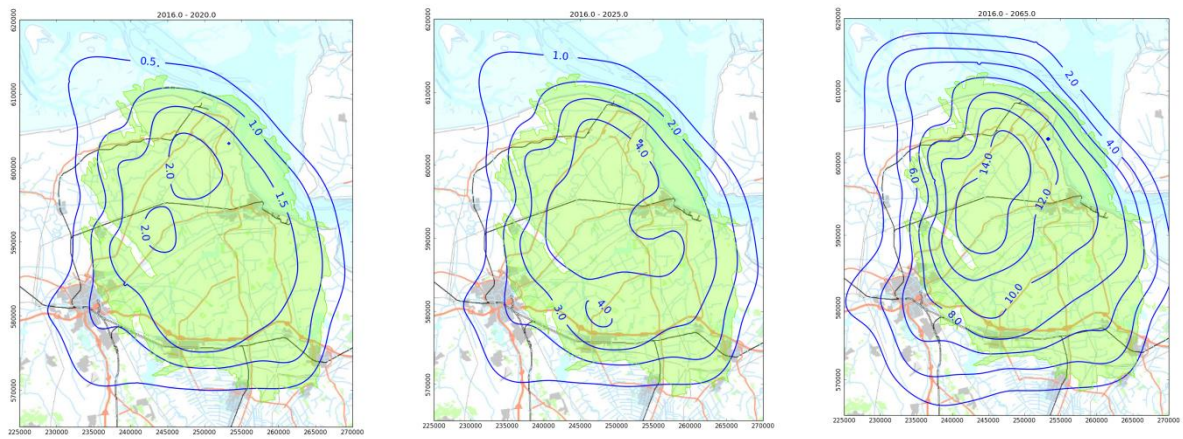

2016-2020	2016-2025	2016-2065

Figure 6-28 Development of future subsidence according to the RTCiM model with 33 BCM annual production

Figure 6-29 shows the results of subsidence models in comparison with the measured subsidence at benchmark 007E0033 near the deepest point of the subsidence bowl.

The parameters used in model realisation A give the best fit with the measurements over the entire time period. The parameters used for realisation B give a reasonable fit, but generally overestimate the measurements and can be considered as the possible upper limit of model realisations. The quality of fit of the models to the data is determined from the fit at all benchmarks.

This spread of models and parameters sufficiently reflects the uncertainty bandwidth of the subsidence forecasts (about 20%). The RTCiM model predicts more subsidence than the Time Decay model (after the end of production). The RTCiM A model was used as basis for the winningsplan. In order to reduce the uncertainty in the future, the subsidence will be monitored closely as described earlier.

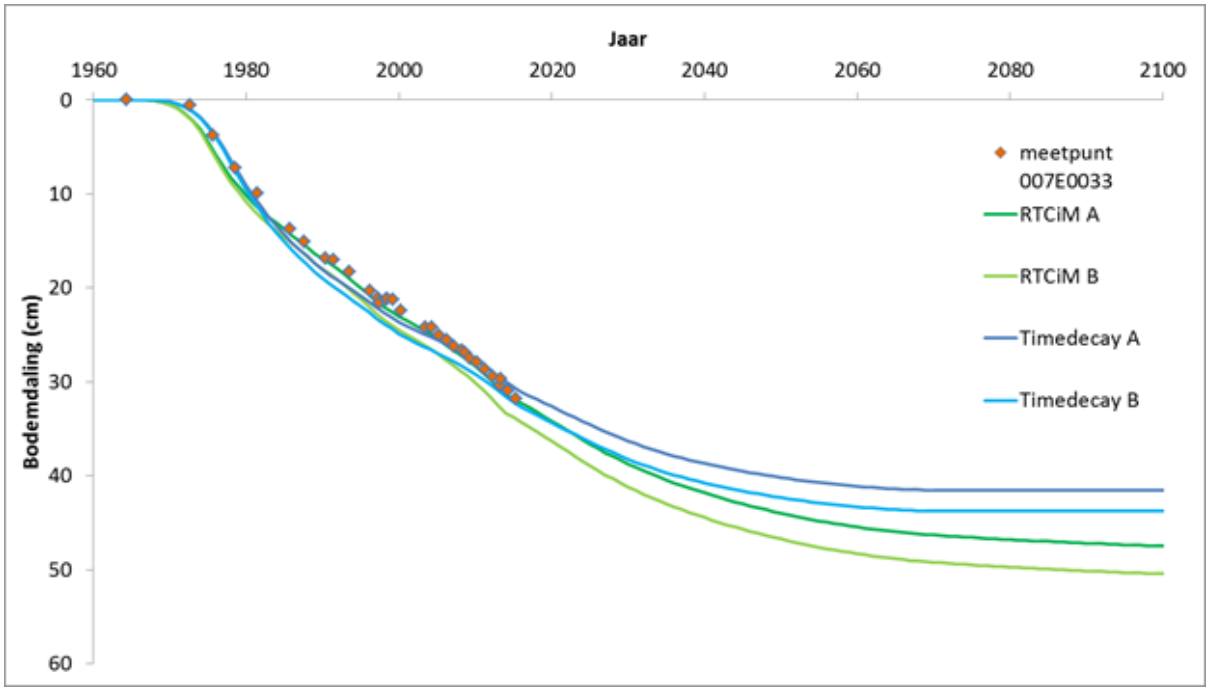

Figure 6-29 Development of subsidence in time at benchmark 007E0033 near the centre of the subsidence bowl.

6.8 Compaction forecast for the hazard calculation

Reservoir compaction is considered to be the main driver for the seismicity in the Groningen field. Chapter 7 describes the seismological model and shows the prediction of the seismic activity rate for the coming 5 years. For this limited time period the compaction forecasted by the base case RTCiM compaction model is compared with the results derived from a linear compaction model. Both models were selected to deliver input to the seismological model. The RTCiM model was described in previous sections. The linear compaction model is using the results from a direct inversion of the subsidence measurements to compaction. A linear function between pressure decrease and this (inverted) compaction was derived and this function was subsequently applied to make a compaction forecast for the coming 5 years. Figure 6-30 shows the forecasted compaction for the coming 5 years (1-1-2016-1-1-2021) for the three production scenarios defined earlier.

A similar comparison is shown in Figure 6-31, but now for the production scenarios that result from an alternative (optimized) spatial offtake.

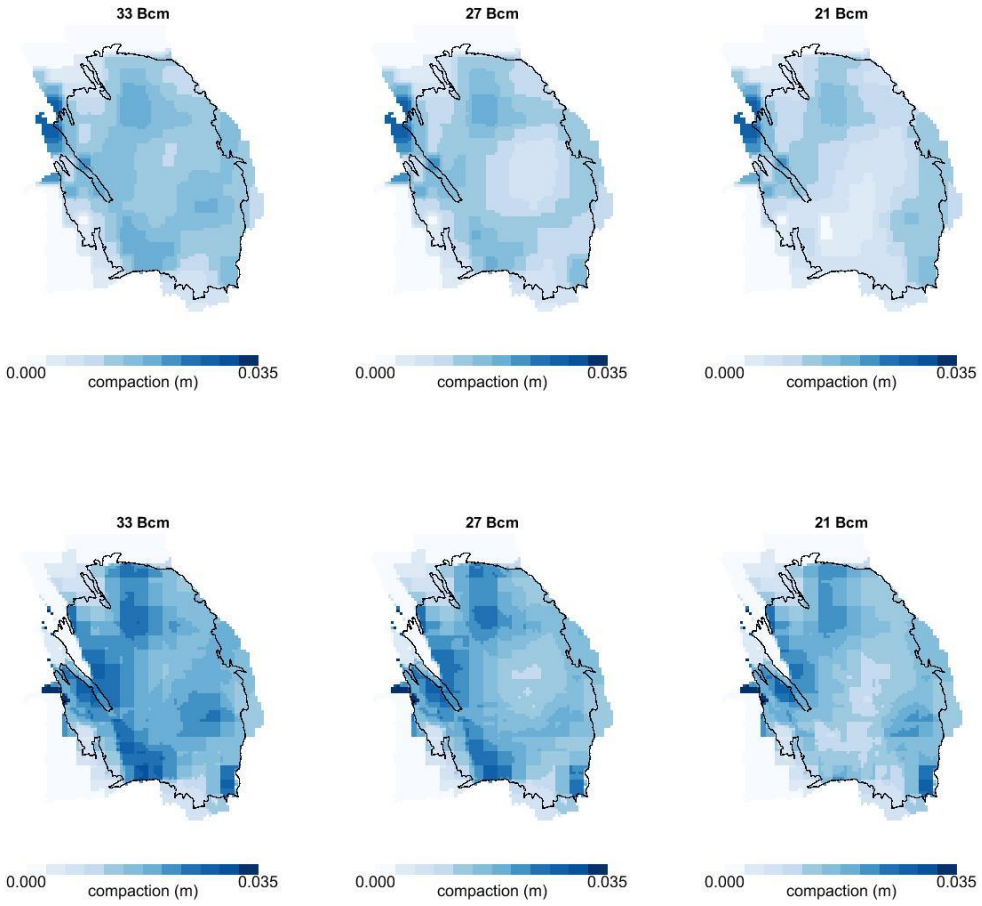

Figure 6-30 Compaction maps based on the linear model (above) and the RTCiM model (below) for the three production scenarios.

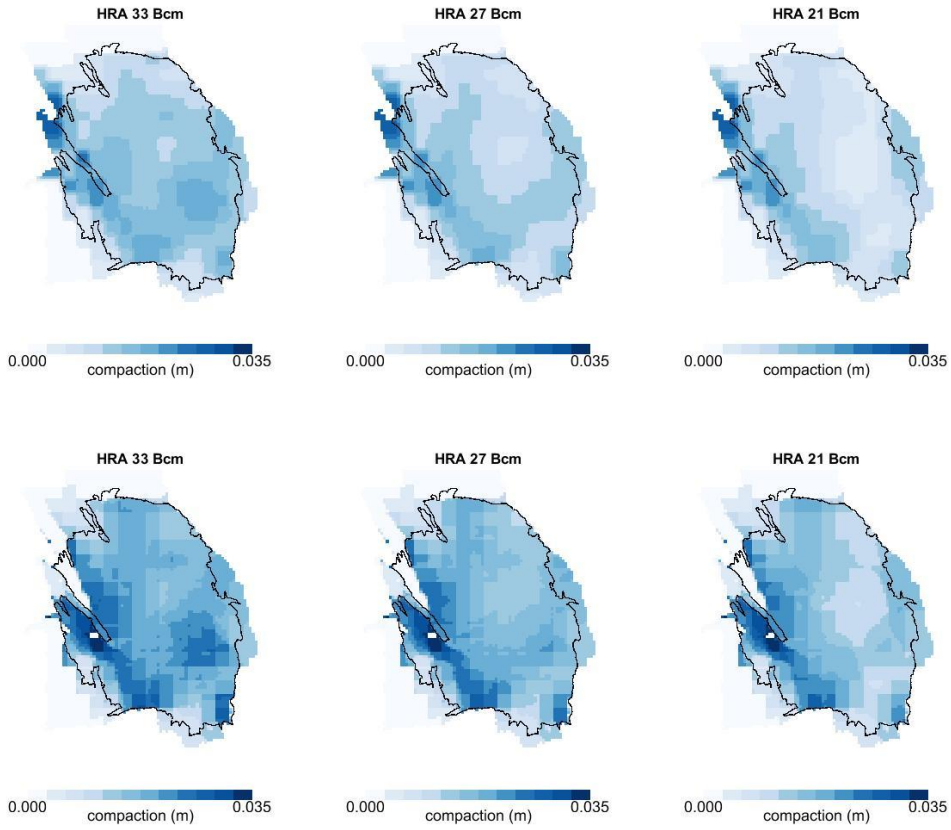

Figure 6-31 *Compaction maps based on the linear model (above) and the RTCiM model (below) for the three alternative (optimized) production scenarios.*